ReScience (R)evolution

Mary Upshall[1,2,3, ID] and Aaron R. Shifman[1,2,3, ID]

[1]Department of Biology, University of Ottawa, Ottawa, Ontario, Canada – [2]uOttawa Brain and Mind Research Institute, Ottawa, Ontario, Canada – [3]Center for Neural Dynamics, University of Ottawa, Ottawa, Ontario, Canada

1 Introduction

This work serves as a replication study of Levitan et al. (2014), where depolarization block is studied in two simplified models (3-dimensional and 2-dimensional) which are proposed reductions of a more complex 5-dimensional model. In vitro, depolarization block has been shown to limit the maximum firing rate of dopaminergic (DA) neurons[1], and is caused by a sustained, large amplitude membrane current[2]. The authors' previous modelling work revealed that a failure to recover from sodium channel inactivation is one way to enter into depolarization block, whereby the availability of sodium channels limits the maximum firing rate of DA cells[3]. Additionally, a slow inactivation (h_s) component of sodium channel had been previously hypothesized[4]. Elaborating on this hypothesis, Levitan et al. (2014) developed a simplified 2D (excluding h_s), and 3D (including h_s) model to analyze the role of a slow inactivating component. Both proposed simplified models successfully reproduced the sodium current measured in DA neurons which had been previously described[5], allowing the authors to faithfully investigate the mechanism of depolarization block. We replicated Figures 1–4 and 6, and in few cases found very minor quantitative differences, as well as two major differences in the results of figure 1c and figure 6.

2 Methods

The methods section should explain how you replicated the original results:
This replication was produced using the model described by Levitan et al. (2014), and personal communication with the authors. While the original study computed all simulations, bifurcation diagrams, and nullclines using XPPAUT, our replication was performed using Python (x.y.z); for full package specifications including version numbers, please see the included requirements.txt. The model description was taken directly from page 1 and 2 of the original paper. Additionally, the model gating variables and the model reductions were taken from Table 1 and page 3 respectively. It should also be noted that in order to get the same result shown in figure 1c we changed the time constant equation for the activation of sodium current (τ_n) for all simulations as follows:

$$\tau_{n^{original}} = 1 + 19e^{-(\frac{\ln[1-0.05(v+40)]}{0.05})^2/300}$$

$$\tau_{n^{modified}} = 1 + 19e^{-(\frac{\ln[1-0.05(v+60)]}{0.05})^2/300}$$
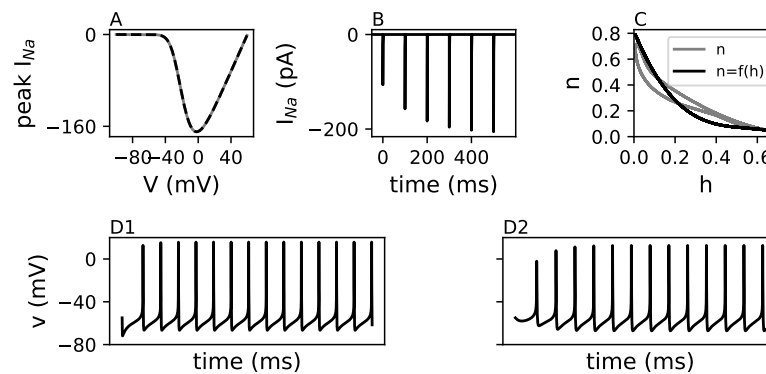
Figure 1. ABC123

As previously mentioned, some further discrepancies were found and will be noted and elaborated on in the discussion section.

3 Results

All figures, with the exception of figure 5 (experimental data), were successfully replicated. Figures 1 and 6 had minor and major discrepancies respectively, which will be addressed accordingly.

In figure 1, the authors show the reliability of their reduced 2/3D models. In figure 1A the authors plotted the peak currents of the models with h_s and without h_s against experimental data from Seutin and Engel (2010) successfully showing that they had not compromised the original sodium current description. Our replication (Figure 1A) shows seemingly identical results for the models with and without h_s. Next, Figure 1B displayed the effect of slow inactivation of sodium current when depolarizing current steps were repeatedly applied. When replicated in Figure 1B, we found that the results were "backwards". This discrepancy will be discussed later. As part of reducing the 5D model, potassium current (n) was modified to a be a function of fast inactivation of sodium current ($f(h)$). This was shown in Figure 1C whereby $f(h)$ and n were plotted against h. In order to successfully replicate figure 1C, the time constant τ_n required modification as shown in the methods section. Figures 1 D1 and 1 D2 compared the 5-D model to the 3-D model respectively. This was well reproduced in our implementation.

Figure 2 analyzed the entry into depolarization with the 2D model (without h_s). Figure 2A demonstrated that applying a current step caused a "ringing" just before entry into depolarization block (stabilized at -19 mV). This same "ringing" was observed in our replication (Figure 2 A), however it was less prominent and was significantly shorter. Figures 2 B1 and B2 were a nullcline analysis of h with an applied current of 0 μA/cm^2 and 3.5 μA/cm^2 respectively. Our replication of both showed identical results.

Levitan et al. (2014) then analyzed the entry into depolarization block with the 3-D model. Figure 3A1 plotted membrane current of the 3-D model followed by an applied current causing depolarization block. They demonstrate that slow inactivation of sodium current provides a mechanism for spike frequency adaptation as opposed to the "ringing" seen with the 2-D model. This was well reproduced in Figure 3 A1. In Figure 3A2 the authors investigated the contribution of h_s to h_{total} ($h_{total} = h_s \times h$) with the same applied current seen in Figure 3A1. This was also well reproduced in Figure 3 A2.

In figures 3B1-B4 the authors also performed a nullcline analysis and outlined the effects
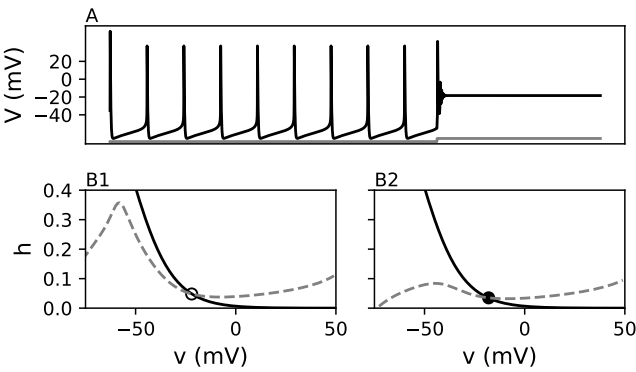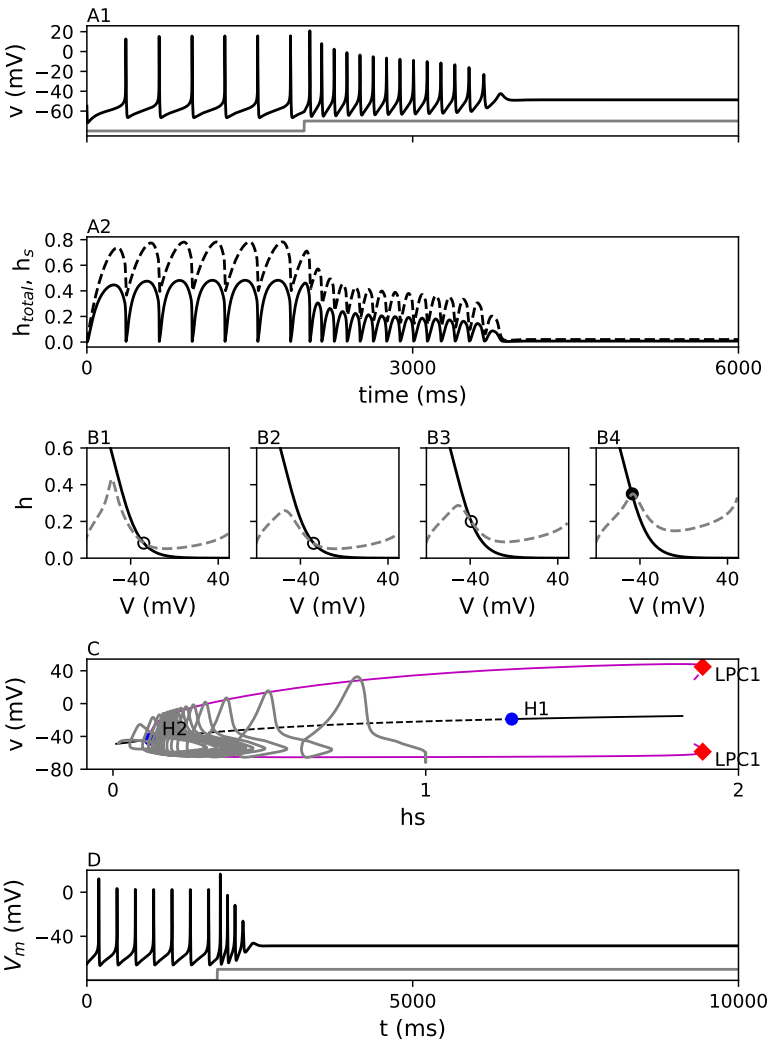
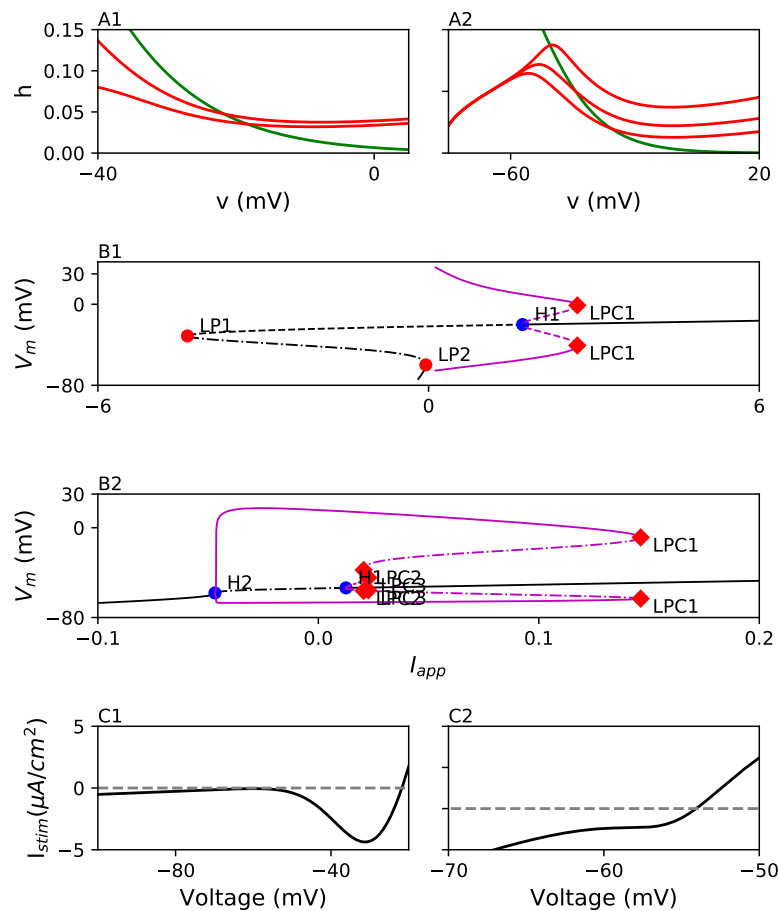**Figure 2**. ABC123

Figure 3. ABC123

Figure 4. ABC123

of varying the current stimulus and h_s in Figures 3 B1-B4. Our results, shown in Figures 3B1 – B4, correspond to the same outcomes faithfully replicate their results. Similarly, Figures 3C and 3D (corresponding to Levitan et al. 2014 Figures 3C and 3D) were well reproduced. 3C was a bifurcation analysis with h_s as the bifurcation parameter overlaid with the trajectory. 3D showed the results of speeding up slow inactivation of sodium current by a factor of 2.

Next, the authors used Figure 4 to compare the differences between the 2-D and the 3-D model, thereby analyzing the significance of the slow inactivation of sodium current. In Figure 4 A1 they summarized the nullcline analysis done in Figure 2B, and Figure 4A2 summarized the analysis performed in Figure 3B . Our results (Figure 4A) were well in accordance with what they had produced. To follow that, Levitan et al. (2014) then compared the bifurcation analysis of the 2D model and 3D model in Figures 4B1 and 4B2 respectively. Our replication (Figure 4B) successfully reproduced the stable oscillation, unstable oscillation, unstable fixed points, and fixed points. Lastly, the original works produced current-voltage (I-V) curves, where Figure 4 C1 was the nonmonotonic IV curve (2-D model), and Figure 4C2 was the monotonic IV curve (3-D model). We had successfully reproduced this by clamping the voltage and computing the membrane current across voltage steps, just as Levitan et al. (2014) had done.

Finally, the authors compared the effects of NMDA and AMPA receptors on entry into depolarization block. As we did not duplicate figure 5, figure 6 corresponds to our figure
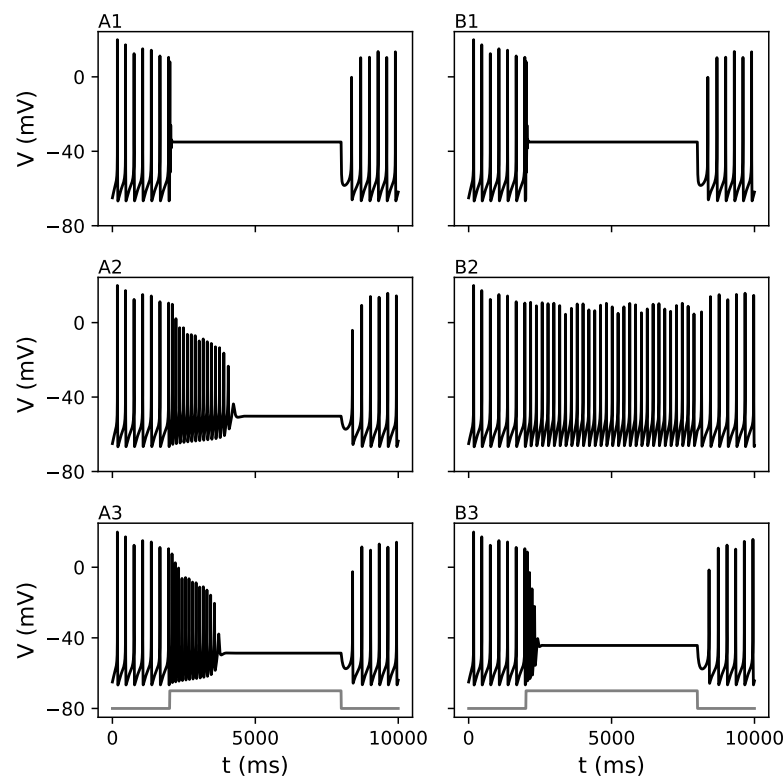
Figure 5. ABC123

5. In Figure 6A1, A2, and A3 they displayed the results coinciding with an applied NMDA conductance, AMPA conductance, or current pulse, respectively. We successfully replicated the current pulse portion of this figure using the 3-D model. However, we found the NMDA and AMPA applied conductance replications to be unsuccessful. After consulting with the authors, we were unable to conclude which parameters had been used and therefore were not able to reproduce these figures. These inconsistencies will be addressed in the discussion section.

4 Discussion

Overall, this implementation replicated the original paper. There were some inconsistencies with the 5-D model (Figure 1) and with the analysis using NMDA and AMPA receptors (Figure 6). More specifically, our replication of Figure 1B was "backwards" where the sodium current decreases towards zero in time, which is opposite in the original implementation. Upon speaking with the authors, they kindly provided us with one of their ODE files for the 3-D model but unfortunately did not have the 5-D model. Hence, we can only speculate that this may have potentially been a graphing error. As previously mentioned, we found some discrepancies with figure 1C which were restored by modifying τ_n (see Methods). The authors' ODE file contained a different set of constants for $f(h)$, however, when we ran the model with the new constants, we found negligible qualitative and quantitative differences. Thus, the modified equation seemed to be the best way to restore the proper model fit given in the original paper. Next, we found that Figure 2A had a shorter and less prominent "ringing" period when entering depolarization block, however the cessation in firing still occurred at -19mV as demonstrated in the original implementation and had identical spikes prior to depolarization

block. Lastly, our findings for Figure 6 were dramatically different from that of the initial implementation. With the provided ODE file, it was unclear which conductances were used in the model. Seeing as the bifurcation analysis replicated in figures 3 and 4 were quantitatively identical, we suspect that the reason Figure 6 was unsuccessfully replicated was due to the fact that the original paper used different parameters.
Despite the subtle discrepancies, this model by far demonstrates all the major results using the 2-D and 3-D model were implemented correctly.

5 Conclusion

With the exception of Figure 6, this implementation confidently shows that the original results were correctly implemented. The subtle discrepancies we had found between the original works and our replication were identified and addressed.

References

1. C. D. Richards, T. Shiroyama, and S. T. Kitai. "Electrophysiological and immunocytochemical characterization of GABA and dopamine neurons in the substantia nigra of the rat." In: **Neuroscience** 80.2 (1997), pp. 545–557.
2. D. Bianchi, A. Marasco, A. Limongiello, C. Marchetti, H. Marie, B. Tirozzi, and M. Migliore. "On the mechanisms underlying the depolarization block in the spiking dynamics of CA1 pyramidal neurons." In: **Journal of Computational Neuroscience** 33.2 (Oct. 2012), pp. 207–225.
3. E. S. Levitan, C. C. Canavier, K. R. Tucker, K. Qian, and N. Yu. "Mathematical analysis of depolarization block mediated by slow inactivation of fast sodium channels in midbrain dopamine neurons." In: **Journal of Neurophysiology** 112.11 (2014), pp. 2779–2790.
4. S. Ding, W. Wei, and F.-M. Zhou. "Molecular and functional differences in voltage-activated sodium currents between GABA projection neurons and dopamine neurons in the substantia nigra." In: **Journal of Neurophysiology** 106.6 (2011), pp. 3019–3034.
5. V. Seutin and D. Engel. " Differences in Na + Conductance Density and Na + Channel Functional Properties Between Dopamine and GABA Neurons of the Rat Substantia Nigra." In: **Journal of Neurophysiology** 103.6 (2010), pp. 3099–3114.